Involvement of Rac in actin cytoskeleton rearrangements induced by MIM-B

Guillaume Bompard[1],*, Stewart J. Sharp[1], Gilles Freiss[2] and Laura M. Machesky[1],‡

[1]School of Biosciences, Division of Molecular Cell Biology, University of Birmingham, Edgbaston, Birmingham, B15 2TT, UK
[2]Inserm U540, Endocrinologie Moléculaire et Cellulaire des Cancers, 60, rue de Navacelles, 34090 Montpellier, France
*Present address: Centre de Recherches en Biochimie Macromoléculaire, FRE 2593 CNRS, 1919, route de Mende, 34293 Montpellier, France
‡Author for correspondence (e-mail: l.m.machesky@bham.ac.uk)

Journal of Cell Science

Summary

Numerous scaffold proteins coordinate signals from the environment with actin-based protrusions during shape change and migration. Many scaffolds integrate signals from Rho-family GTPases to effect the assembly of specific actin structures. Here we investigate the mechanism of action MIM-B (missing in metastasis-B) on the actin cytoskeleton. MIM-B binds actin monomer through a WASP homology 2 motif, bundles actin filaments via an IRSp53/MIM domain, and is a long isoform of MIM, a proposed metastasis suppressor. We analysed the activity of MIM-B toward the actin cytoskeleton as well as its potential link to cancer metastasis. Endogenous MIM-B protein is widely expressed and its expression is maintained in various metastatic cell lines. MIM-B induces lamellipodia-like actin-rich protrusions. The IRSp53/MIM domain of MIM-B, as well as Rac activity are required to induce protrusions, but not the WASP homology 2 motif. MIM-B binds and activates Rac via its IRSp53/MIM domain, but this is not sufficient to induce lamellipodia. Finally, our data revealed that actin bundling and Rac-binding properties of MIM-B are not separable. Thus, MIM-B is unlikely to be a metastasis suppressor but acts as a scaffold protein that interacts with Rac, actin and actin-associated proteins to modulate lamellipodia formation.

Supplementary material available online at
http://jcs.biologists.org/cgi/content/full/118/22/5393/DC1

Key words: Actin cytoskeleton, Lamellipodia, Rho GTPases, Rac, Bundling

Introduction

The actin cytoskeleton plays a key a role in regulating essential cellular processes such as motility, cytokinesis and vesicular trafficking. The driving force of these processes depends on the dynamic remodelling of the actin cytoskeleton through assembly, disassembly and organisation of actin filaments into functional networks. For example, at the leading edge of migrating cells, lamellipodia, which are broad, sheet-like protrusive structures, are composed of short-branched filaments, whereas filopodia, which are thin needle-like projections, are composed of bundles of long parallel actin filaments. Membrane ruffles can also be observed at the leading edge of cells when non-adherent lamellipodia fold back over the dorsal surface. These structures are fundamental for cell motility, at least in culture, and are regulated by various actin-monomer-binding and actin-filament-binding proteins (Paavilainen et al., 2004; Pollard and Borisy, 2003).

Actin-monomer-binding proteins such as profilin and the WASP family of proteins can stimulate actin polymerisation respectively at the barbed-end of filaments or de novo through activation of the Arp2/3 complex (Paavilainen et al., 2004; Pollard and Borisy, 2003). Some actin-monomer-binding proteins, like β-thymosins, inhibit actin polymerisation by sequestering ATP-actin monomers (Paavilainen et al., 2004). A similar dual effect is also observed with many actin-filament-binding proteins (Revenu et al., 2004). The activity of these

proteins is mainly orchestrated by the Rho family of GTPases, notably Cdc42 and Rac, which promote the formation of filopodia and lamellipodia, respectively (Etienne-Manneville and Hall, 2002). Scaffold proteins also play a key role by coordinating various aspects of actin dynamics. IRSp53, for example, binds Rac and WAVE/SCAR-2 and probably promotes actin assembly (Miki et al., 2000). Furthermore, IRSp53 has been shown to bind directly to Eps8 in a Rac-GEF complex containing Abi-1 and SOS-1 (Funato et al., 2004). Those interactions promote Rac activation and are proposed to provide a specific Rac effector function for motility and cancer cell invasion. Similarly, Tiam1, a Rac-GEF, has been recently shown to enhance the signalling specificity of IRSp53 toward Rac effects on actin cytoskeleton by inducing complex formation between IRSp53, activated Rac and WAVE/SCAR-2 (Connolly et al., 2005). Cortactin, also implicated in cancer cell migration, binds to N-WASP, filamentous actin and the Arp2/3 complex and plays a key role in the assembly of branched actin networks in lamellipodia (Daly, 2004). Thus, a variety of scaffold proteins connect signalling to actin dynamics.

We recently identified a new actin-monomer-binding protein: MIM-B (Woodings et al., 2003). MIM-B is a long isoform of MIM (missing in metastasis), a proposed suppressor of metastasis in bladder cancer (Lee et al., 2002). The N-terminal 254 residues of MIM-B form a conserved domain,

IRSp53/MIM domain (IMD), able to bind to and bundle actin filaments (Yamagishi et al., 2004). We recently determined the structure of the IMD of IRSp53, which forms a zeppelin-shaped dimer possessing an actin-filament-binding site at each extremity (Millard et al., 2005). As mentioned, MIM-B also binds actin monomer through a WASP homology 2 (WH2) motif located at its C-terminal end (Mattila et al., 2003; Woodings et al., 2003). A proline-rich region is located upstream of this domain and has recently been shown to interact with cortactin (Lin et al., 2005). Finally, this proline-rich region is preceded by a sequence that we, and others, have found to interact with the receptor protein tyrosine phosphatase RPTP∂ (Gonzalez-Quevedo et al., 2005; Woodings et al., 2003). Overexpression of MIM-B in various cell lines induces actin-rich membrane protrusions, microspikes and also loss of stress fibres (Gonzalez-Quevedo et al., 2005; Mattila et al., 2003; Woodings et al., 2003). Thus, MIM-B is a good candidate for a scaffold protein involved in actin dynamics.

Additionally, MIM-B expression is regulated by Sonic hedgehog (Shh) and MIM-B expression increases during development in the hair follicles of skin as well as in basal cell carcinomas induced by Shh expression (Callahan et al., 2004). This regulation suggests that levels of MIM-B are likely to be controlled during developmental programmes in various tissues and also that MIM-B expression may be altered in cancer cells, leading to changes in the signalling and architecture of the cytoskeleton.

In this study, we address the nature of MIM-B interaction with the actin cytoskeleton in general and with the GTPase of the Rho family in particular, as well as its potential link to cancer metastasis. We find that MIM-B is widely expressed and its expression maintained in various metastatic cell lines. MIM-B activity towards the actin cytoskeleton requires its IMD and Rac interaction. We demonstrated that MIM-B binds and activates Rac through its IMD. By developing a bundling-deficient mutant of MIM-B, we showed that actin filament bundling and Rac activation are two exclusive MIM-B activities.

Collectively, our data show that MIM-B induces actin-rich membrane protrusions through the activation of Rac, potentially acting as a scaffold protein to recruit Rac effectors and organise actin assembly. Our data also suggest overlap (or crosstalk) between the binding sites for Rac and for F-actin and may force us to rethink previous proposals for the Rac-binding site on the related IMD of IRSp53 (Millard et al., 2005).

Materials and Methods
Reagents and antibodies
All chemicals were purchased from Sigma unless otherwise stated and restriction enzymes from New England Biolabs. Monoclonal antibody against myc epitope (9E10) was purchased from Cancer Research UK. Monoclonal anti-α-tubulin (T9026), polyclonal anti-HA (H6908) and TRITC-phalloidin were from Sigma. Monoclonal anti-Rac antibody (23A8) was purchased from Upstate. Goat FITC-conjugated anti-mouse Ig was from Jackson Laboratories.

DNA constructs and site directed mutagenesis
Constructions encoding myc or HA-tagged IMD (amino acids 1-254), MIM-B Δ234 (aa 235-759), MIM-B ΔIMD (aa 260-759), MIM-B ΔWH2 (aa 1-727) or MIM-B ΔCt (1-598) were generated by PCR-based cloning into BamHI-EcoRI restriction sites from pRK5myc or HA vectors. The bacterial expression construct pRSET-IMD encoding His-tagged IMD was generated by PCR based cloning into BamHI-EcoRI restriction sites from pRSET vector (Invitrogen).

Site-directed mutagenesis of F-actin binding site within the IMD sequence was performed by PCR. The changed bases are underlined and only sequences of the forward oligonucleotides are given. The oligonucleotide used for introducing K149,150,152,153D (K4D) mutations was 5′-CTG AAA CTG CAG GAC GAC GCA GAC GAC GTG G-3′. Mutated IMD cDNA was then cloned into pRK5myc as described previously. The BamHI-BglII fragment from pRK5myc-MIM-B was substituted by the corresponding fragment from pRK5myc-IMD K4D generating pRK5myc-MIM-B K4D. Finally, pRK5myc-IMD K4D was used as template to generate pRSET-IMD K4D as previously described. DNA sequencing of all constructs was performed by the University of Birmingham Functional Genomics Laboratory.

Vectors encoding FLAG-tagged N17-Rac or N17-Cdc42 (pRK5FLAG-N17-Rac or N17-Cdc42), GST-tagged N17 or -L61-Rac or -Cdc42 (pGEX2T-N17 or L61-Rac or -Cdc42), myc-tagged human IRSp53 (pRK5myc-IRSp53) and HA-tagged constitutively active (DH-PH) mouse Vav1 (pRK5HA-Vav) were a generous gift from Alan Hall (LMCB-UCL, London).

Generation and purification of MIM-B antibodies
The peptides CSALGGLFQTISDMKGSYPV (aa 9-29), CEEWKK-VANQLDKDHAKEYKK (aa 113-132), CKLQKKAKKVDTLGRG-DIQPQ (aa 146-165) and CDVNDKYLLLEETEKQAVRKA (aa 172-191) were synthesised (Alta Biosciences, Birmingham, UK) and coupled to maleimide-activated keyhole limpet haemocyanin (Pierce, Rockford, IL) according to the manufacturer's instructions. Two rabbits were immunised with each of the coupled peptides (Eurogentec, Belgium) and MIM-B antibodies were affinity purified from final rabbit serum using recombinant His-tagged IMD immobilised on western blot strips (Pollard, 1984).

Cell culture
COS-7, Swiss3T3, MDA-MB231 and MDA-MB486 cells were cultured in Dulbecco's Modified Eagle's medium (DMEM) supplemented with 10% foetal bovine serum (FCS) and antibiotics. MCF7 and PC3 cells were maintained in Ham's F-12/DMEM (1:1) supplemented with 10% foetal calf serum (FCS) and antibiotics. RT4, RT112, T24, TccSup, J82, DAG-1 cells, a generous gift from Pierre Champelovier (CHU de Grenoble, Grenoble, France) and LNCaP cells, were maintained in RPMI supplemented with 10% FCS and antibiotics. COS-7 cells were transfected using Gene Juice (Novagen) according to the manufacturer's instructions. Swiss 3T3 cells were serum starved and microinjected as previously described (Machesky and Hall, 1997).

Preparation of mouse tissue extracts and lysates from cancer cell lines
Tissues isolated from adult Swiss and C57BL mice were washed in ice cold PBS and homogenised using a Dounce homogeniser in tissue buffer: 25 mM HEPES, pH 7.6, 150 mM NaCl, 1 mM EDTA, 1% Triton X-100, 1 mM PMSF, CLAP (chymostatin, leupeptin, antipain and pepstatin at a final concentration of 0.1 μg/ml of each). Lysates were clarified by centrifugation at 21,000 g for 60 minutes at 4°C.

RT4, RT112, T24, TccSup, J82, DAG-1, LNCaP, PC3, MCF7, MDA MB486 and MDA MB231 cells were lysed in Tissue buffer and lysates clarified by centrifugation at 16,000 g for 10 minutes at 4°C. Protein concentrations were then measured using the BioRad protein assay.

Immunofluorescence

Cells were stained and mounted on glass slides as previously described (Machesky and Hall, 1997). In brief, 18 hours after transfection or 2 hours after microinjection, cells were fixed with 4% formaldehyde in PBS, blocked in 50 mM NH$_4$Cl in PBS, permeabilized in 0.1% Triton X-100 in PBS and stained with phalloidin or the appropriate antibodies in PBS containing 0.2% gelatin.

Rac pull-down assays

24 hours post-transfection, COS-7 cells in 35 mm dishes were starved of serum overnight. Cells were washed twice with ice-cold PBS and lysed into GTPase lysis buffer (10 mM Tris-HCl pH 7.3, 150 mM NaCl, 1 mM EGTA, 1 mM EDTA, 1% NP-40, 0.5% Octyl-β-glucopyranoside, 10 mM MgCl$_2$, 1 mM Na$_3$VO$_4$, 1 mM PMSF, CLAP). Lysates were cleared by centrifugation at 16,000 **g** for 5 minutes at 4°C, an aliquot saved to assess total Rac levels, and the remaining lysates applied onto 20 μg of 50% slurry of PAK-CRIB coupled to glutathione-agarose beads for 60 minutes at 4°C. Beads were washed three times with ice-cold GTPase lysis buffer and Rac activation was determined by immunoblot using monoclonal Rac antibody. Expression of various constructs was subsequently determined after stripping and probing with monoclonal anti-myc or polyclonal anti-HA antibodies. Each experiment has been at least repeated three times.

Protein expression and purification

pRSET-IMD wt and K4D were transformed into *E. coli* BL21-AI™ (Invitrogen). Cultures were grown at 37°C to OD$_{600}$ 0.6 and protein expression was induced with 0.2% arabinose for 3-4 hours at 37°C. Cells were washed in ice-cold PBS, resuspended in S buffer (50 mM sodium phosphate pH 8, 20 mM Tris-HCl pH 8, 250 mM NaCl, 5 mM imidazole, 1 mM PMSF, CLAP) and sonicated. The cleared sonicate was then passed twice over a TALON metal affinity column (BD Biosciences). The column was washed once with S buffer and twice with W buffer (20 mM Tris-HCl pH 8, 250 mM NaCl, 30 mM imidazole). Proteins were eluted in E buffer (20 mM Tris-HCl pH 8, 100 mM NaCl, 150 mM imidazole), dialysed against 20 mM Tris-HCl pH 8 with 100 mM NaCl, and concentrated to a minimum of 130 μM using Vivaspin 15R concentrator (Vivascience, Hannover, Germany).

pGEX2T N17-Rac, L61-Rac, N17-Cdc42 or L61-Cdc42 encoding the corresponding GTPase fused to GST were transformed into *E. coli* BL21 (DE3). Protein expression was induced with 1 mM IPTG for 3 hours at 37°C. Bacteria were resuspended in PBS/1% Triton X-100 containing 1 mM PMSF and CLAP, and sonicated. Proteins were purified by applying the cleared sonicate onto a glutathione-agarose column. The column was then extensively washed with PBS/1% Triton X-100.

Pull-down experiments

A 35 mm dish of transfected COS-7 cells was lysed in low-salt tissue buffer (50 mM NaCl). 150 μg cleared lysates were incubated for 60 minutes at 4°C with 20 μg recombinant GST-GTPases immobilised on glutathione-agarose beads. Beads were washed four times with tissue buffer and binding evaluated by immunoblotting with monoclonal anti-myc antibody. Pull down of endogenous MIM-B was similarly performed using 2 mg mouse brain extract prepared as described. Direct binding of the IMD of MIM-B to the GTPases was performed by incubating 3 μg of recombinant GST-GTPases immobilised on glutathione-agarose beads with 9 μg recombinant His-tagged IMD wt or K4D in tissue buffer. All pull downs were repeated independently three times.

F-actin binding and actin bundling assays

F-actin binding and bundling assays were performed as previously described (Millard et al., 2005). The effect of GTPases on bundling activity was determined as follows. Immobilised GST-GTPases purified as previously described were incubated overnight at 4°C in thrombin buffer (150 mM NaCl, 50 mM Tris-HCl pH 8.0, 5 mM MgCl$_2$, 2.5 mM CaCl$_2$, 1 mM DTT) containing 10 U thrombin (Calbiochem). Thrombin-cleaved GTPases were eluted and dialysed into 20 mM Tris-HCl pH 8.0, 100 mM NaCl and concentrated to ~230 μM using a Vivaspin 15R concentrator. Recombinant His-tagged IMD (5 μM) was incubated with a range of concentrations (1-10 μM) of GTPases in F buffer (2 mM Tris-HCl, pH 8.0, 0.2 mM ATP, 0.5 mM DTT, 0.2 mM CaCl$_2$, 50 mM KCl, 2 mM MgCl$_2$ and 0.1 mM EGTA) for 30 minutes on ice followed by 30 minutes at room temperature. F-actin (5 μM) was then added and bundling assay was performed as described (Millard et al., 2005).

Dimerisation of MIM-B

35 mm dishes of COS-7 cells were co-transfected with pRK5HA-MIM-B and pRK5myc-IMD wt or K4D. 36 hours after transfection, cells were lysed in 50 mM Tris-HCl pH 7.5, 150 mM NaCl, 1 mM EDTA, 1% Triton X-100, 10% glycerol, 1 mM Na$_3$VO$_4$, 10 mM NaF, 1 mM PMSF, CLAP. Cleared lysates were incubated with protein-G coupled to agarose beads (Cancer Research UK) for 30 minutes at 4°C. Clarified lysates were then incubated with 5 μg of monoclonal anti-myc antibody for 60 minutes at 4°C and then protein-G was added followed by a 30 minute incubation at 4°C. Beads were washed four times with lysis buffer and binding of IMDs to HA-MIM-B was analysed by immunoblotting using polyclonal ant-HA antibody. Expression and immunoprecipitation of myc-IMDs were determined after stripping and probing with monoclonal anti-myc antibody.

Results

MIM-B is widely expressed and its expression is maintained in various metastatic cell lines

To study expression of endogenous MIM-B protein, we developed a polyclonal antibody directed against four peptides of the IMD sequence of MIM-B (Fig. 1). The antibody was affinity purified using recombinant His-tagged IMD immobilised on western blot strips (Pollard, 1984). In mouse brain extract, anti-MIM-B antibody specifically recognised a protein of ~116 kDa, the expected MIM-B molecular mass which appears as a doublet in this tissue (Fig. 2A, left panel). Such a doublet has also recently been observed with different MIM-B antibodies (Gonzalez-Quevedo et al., 2005). This protein was also specifically immunoprecipitated with the anti-MIM-B antibody but not the pre-immune serum (Fig. 2A, left panel). It is interesting to note that the fast-running form of
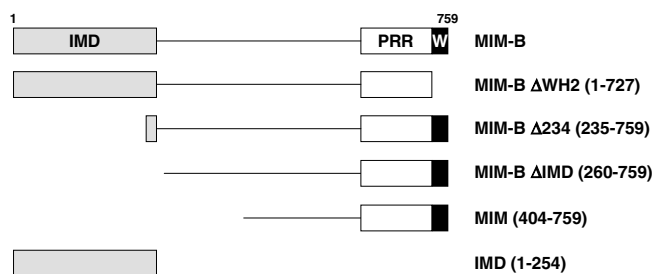

Fig. 1. Schematic representation of the MIM-B expression constructs used in this study. Protein segments are indicated within parentheses. IMD, IRS/MIM domain; PRR, proline-rich region; W, WASP homology 2 domain (WH2).

MIM-B was not immunoprecipitated in these conditions. This form could correspond to a post-translationally modified form of MIM-B which is not recognised by anti-MIM-B antibody in its native state or which is particularly labile. To further test the specificity of our antibody, we tested it against various myc-tagged MIM-B proteins and only those carrying the epitope are specifically recognized (Fig. 2A, right panel). The expression of tagged proteins was confirmed by anti-myc antibody immunoblot (Fig. 2A, right panel). These results clearly demonstrate the specificity of the anti-MIM-B antibody.

Fig. 2. MIM-B protein is widely expressed and is not downregulated in metastatic cell lines. (A) Characterisation of anti-MIM-B antibody. (Left) Lysates from mouse brain (L) were used to immunoprecipitate endogenous MIM-B using pre-immune serum (PI) or affinity-purified anti-MIM-B antibody (Pur) and analysed by immunoblotting with anti-MIM-B antibody. (Right) Lysates from COS-7 cells transfected with constructs expressing myc-MIM-B, myc-MIM-B ΔIMD (ΔIMD) or myc-IMD (see Fig. 1) were analysed by immunoblotting with anti-MIM-B antibody and reprobed with anti-myc antibody. Positions of molecular size markers are indicated in kDa. (B) Tissue distribution of MIM-B. 50 μg lysates from various mouse tissues were separated on SDS-PAGE and analysed by immunoblotting with anti-MIM-B antibody. SK, skeletal. (C) MIM-B expression is not downregulated in metastatic cell lines. Expression of endogenous MIM-B was studied by immunoblotting with anti-MIM-B antibody in non-metastatic (–) or metastatic (+) cell lines from bladder (top), prostate or breast (bottom). Tubulin was subsequently probed as a loading control. This result is representative of three independent experiments.

Unfortunately this antibody appeared unsuitable for immunofluorescence studies (data not shown).

The transcript of mouse MIM-B was previously detected in liver, kidney and heart and at lower levels in lung, spleen and brain (Mattila et al., 2003). To investigate the expression of endogenous MIM-B protein, extracts from various mouse tissues were prepared and analysed by immunoblotting with anti-MIM-B antibody. Endogenous MIM-B protein was detected in brain, lung, liver, bladder and spleen (Fig. 2B). However, we could not detect any expression of MIM-B in kidney, intestine, heart and skeletal muscle (Fig. 2B). The partial discrepancy between the two results could simply be due to the lack of complete correlation between mRNA and protein levels.

MIM, one variant of MIM-B, which corresponds to the C-terminal 355 residues (Fig. 1), has been proposed to be a metastasis suppressor. MIM mRNA is downregulated in certain metastatic bladder and prostate cancer cell lines (Loberg et al., 2005; Nixdorf et al., 2004, Lee et al., 2002). Using the anti-MIM-B antibody, we studied the expression of endogenous MIM-B protein in various non-metastatic and metastatic cell lines. Immunoblot analysis revealed no significant expression differences of MIM-B in non-metastatic RT4 and RT112, and metastatic T24, TccSup, J82 and DAG-1 bladder cell lines (Fig. 2C, top). We extended this study to various cancer cell lines, and obtained similar results using non-metastatic LNCaP or metastatic PC3 prostate cell lines and non-metastatic MCF7 or metastatic MDA-MB231 or -MB486 breast cell lines (Fig. 2C, bottom). These results clearly demonstrate that the expression of MIM-B protein is not affected by the metastatic status of cells. Supporting this idea is the fact that MIM-B mRNA is also elevated in the metastatic PC3 over the non-metastatic LNCaP prostate cancer cell lines (Loberg et al., 2005). Our study does not address whether the shorter MIM isoform is downregulated in metastatic cells however, because this isoform cannot be recognised by our anti-MIM-B antibody.

MIM-B induces actin-rich membrane protrusions in serum-starved Swiss 3T3 cells

We previously showed that MIM-B overexpression in various cell lines induces actin cytoskeletal rearrangements characterised by the induction of actin-rich protrusions resembling microspikes and lamellipodia at the plasma membrane (Woodings et al., 2003). MIM-B binds and bundles F-actin through its N-terminal IMD (Yamagishi et al., 2004), and binds actin monomer through its C-terminal WH2 motif (Mattila et al., 2003; Woodings et al., 2003). In order to define which MIM-B domains are involved in actin-cytoskeletal rearrangements, we microinjected serum-starved quiescent Swiss 3T3 cells with various MIM-B expression constructs (Fig. 1). In these conditions, Swiss 3T3 cells have very few stress fibres or lamellipodia (Machesky and Hall, 1997). Expression of full-length MIM-B results in the induction of actin-rich membrane protrusions that look like ruffles or
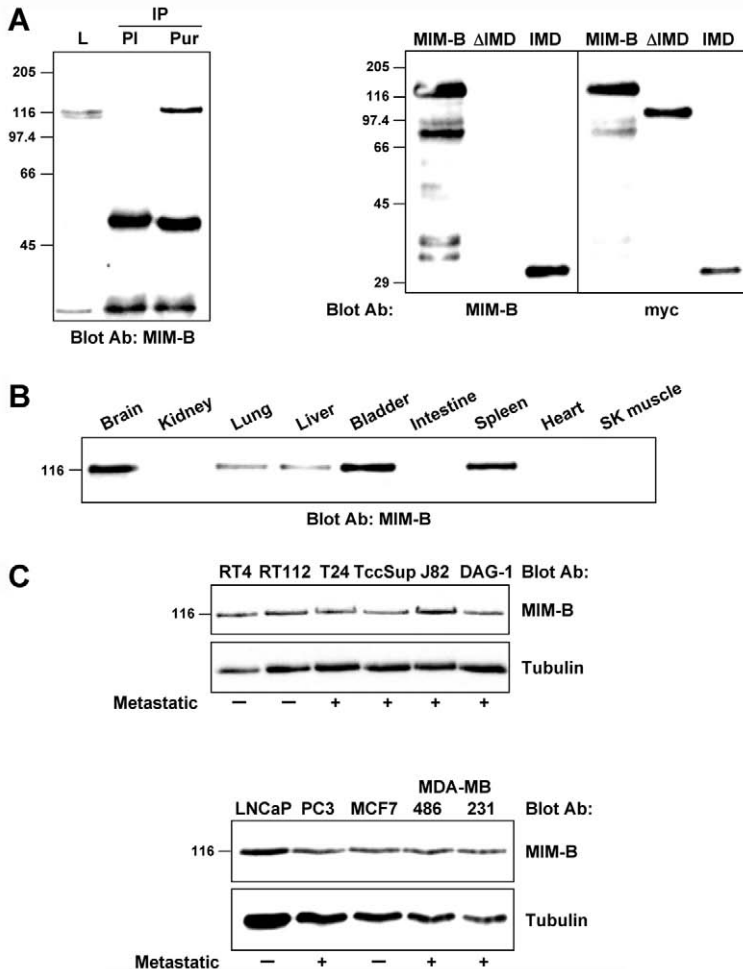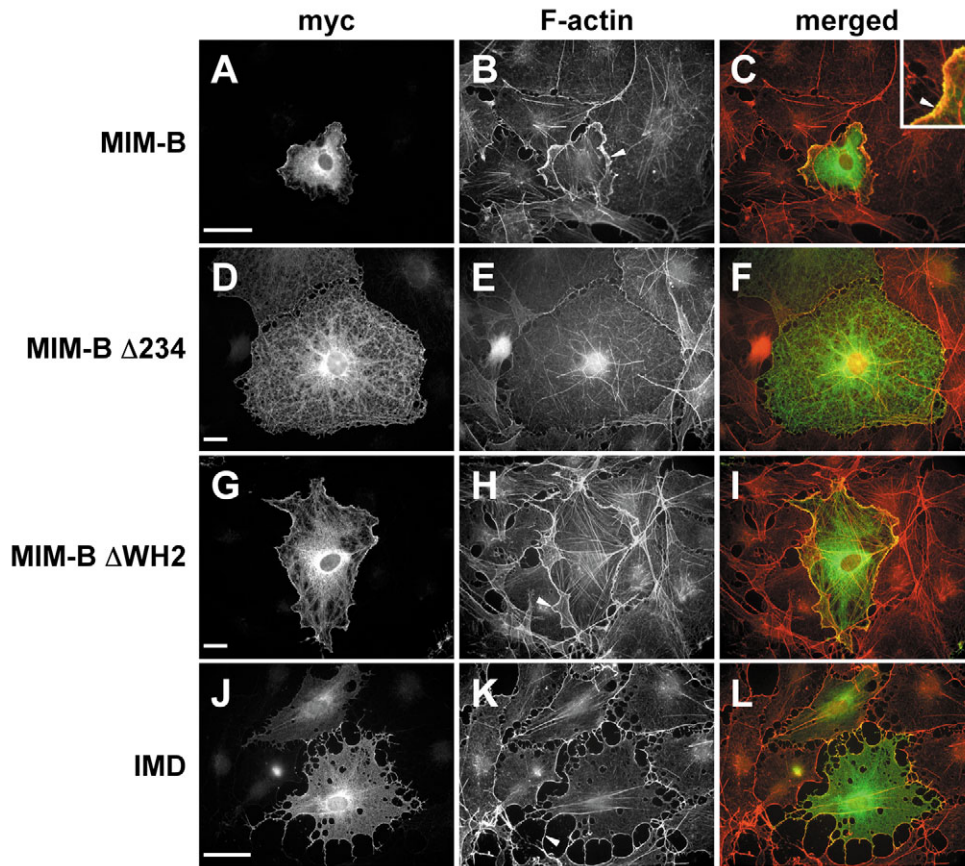
Fig. 3. The IMD of MIM-B is required for MIM-B-induced actin-rich membrane protrusions in serum-starved Swiss 3T3 cells. Constructs (see Fig. 1) encoding myc-MIM-B (A-C), myc-MIM-B Δ234 (D-F), myc-MIM-B ΔWH2 (G-I) or myc-IMD (J-L) were microinjected into serum-starved quiescent Swiss 3T3 cells. Cells were treated for indirect FITC (green) localisation of MIM-B constructs with anti-myc antibody (A,D,G,J) and F-actin with TRITC-coupled (red) phalloidin (B,E,H,K). Merged images (C,F,I,L) are presented. Boxed image in C is an enlargement of the merged image. Bar, 20 μm.

lamellipodia (Fig. 3B arrowhead). MIM-B is enriched at the edge of these actin structures (Fig. 3C enlargement, arrowhead). Deletion of a large part of the IMD (MIM-B Δ234) greatly reduces the MIM-B effect on the actin cytoskeleton (Fig. 3D-F) however deletion of the WH2 motif does not have noticeable consequences (Fig. 3G-I, arrowhead). Expression of the IMD alone induces a spiky appearance that could result from active protrusion and/or retraction of the cell periphery, but does not induce lamellipodia formation (Fig. 3J-L, arrowhead) (see also Yamagishi et al., 2004).

## MIM-B effect towards the actin cytoskeleton requires Rac activity

Actin-rich membrane protrusions induced by MIM-B in serum-starved Swiss 3T3 cells look like ruffles and lamellipodia, structures generally observed following the activation of the small GTPase Rac (Etienne-Manneville and Hall, 2002; Hall, 1998) In order to investigate a potential role of Rac in MIM-B activity toward the actin cytoskeleton, we co-microinjected serum-starved Swiss 3T3 cells with constructs expressing myc-tagged MIM-B and FLAG-tagged dominant-negative mutants (N17) of either Rac or Cdc42. Lamellipodia induced by MIM-B are completely inhibited by coexpression of N17-Rac mutant, but most of the expressing cells showed a spiky appearance similar to the example shown here (Fig. 4A-C, two independent experiments, >10 cells each, no lamellipodia). N17-Cdc42 did not inhibit the lamellipodia or the spiky appearance (Fig. 4D-F, arrowhead, two

independent experiments, 20 cells each, >80% cells with lamellipodia and protrusions). This result demonstrates that Rac activity plays a key role in MIM-B-induced lamellipodia formation. However, N17Rac or N17Cdc42 did not alter the phenotype of serum-starved quiescent Swiss 3T3 cells expressing MIM-B IMD (supplementary material Fig. S1). Together, our results suggest that Rac mediates MIM-B-induced lamellipodia formation, but not IMD-induced spike formation. As in serum-starved conditions, the activity of Rho-GTPases is greatly reduced (Hall, 1994), it seemed likely that MIM-B could activate Rac.

## The IMD domain of MIM-B is necessary and sufficient to activate Rac

To study the effect of MIM-B on the activity of Rac, GTP-loaded Rac was specifically pulled down, using the CRIB domain of PAK fused to GST, from COS-7 cells overexpressing MIM-B. A constitutively active form (DH/PH) of the mouse GTP exchange factor (GEF) Vav1, an activator of Rac, was used as a positive control. MIM-B overexpression significantly stimulated Rac activity compared to mock transfected cells (Fig. 5A). In contrast, the small isoform MIM (Lee et al., 2002), which does not have any effect on the actin cytoskeleton (Woodings et al., 2003), has only a minor effect on Rac activity even if its expression is greater than MIM-B (Fig. 5A). This result clearly demonstrates that MIM-B is a Rac activator, and that activation requires the first 403 residues of MIM-B.

Fig. 4. Involvement of Rac but not Cdc42 in MIM-B-induced actin cytoskeletal reorganisation. A construct encoding myc-MIM-B was co-microinjected with constructs expressing either the FLAG-tagged dominant negative form of Rac (N17 Rac, A-C) or Cdc42 (N17 Cdc42, D-F). Cells were treated as described in Fig. 3. Bar, 20 μm.
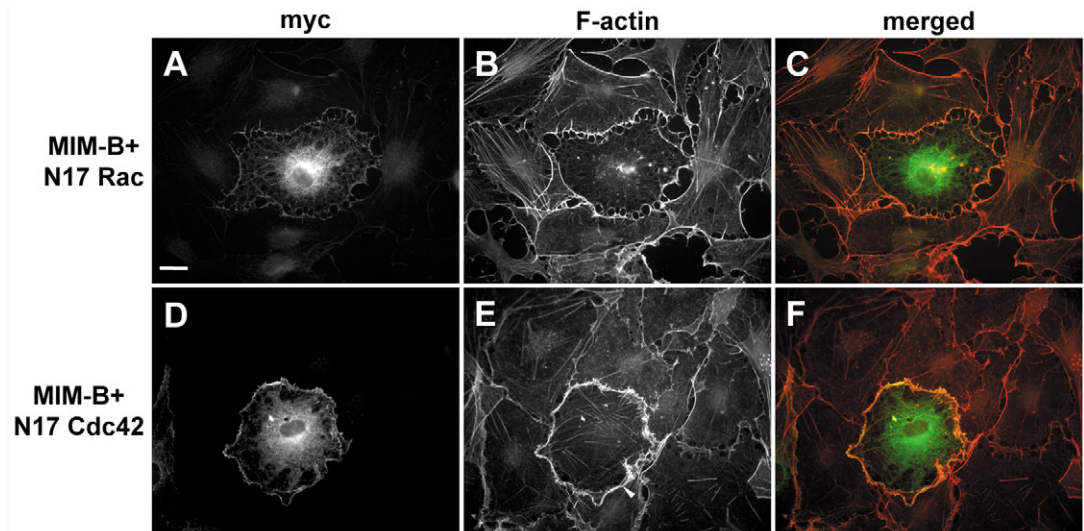
We used the same approach to define the minimal sequence of MIM-B involved in the activation of Rac. Various MIM-B mutants were expressed in COS-7 cells and their effect on Rac activity determined. Deletion of the IMD domain of MIM-B completely abolished Rac activation (Fig. 5B). Inversely, the IMD on its own stimulates Rac activity to a similar level as the full-length protein (Fig. 5B) demonstrating that the IMD is necessary and sufficient to activate Rac. In order to define whether this property was specific among IMD proteins to MIM-B, we studied the effect of IRSp53 overexpression, on Rac activity. Compared to mock-transfected cells (Fig. 5A) and at similar expression levels, MIM-B is greatly more efficient in activating Rac than IRSp53 (Fig. 5C), confirming a recent observation showing that IRSp53 does not activate Rac when overexpressed alone (Funato, 2004). Furthermore, these data demonstrate that activation of Rac by IMD containing proteins is not a conserved property. Thus, the stimulation of Rac activity by MIM-B is mediated by its IMD and Rac activation by the IMD is necessary, but does not appear to be sufficient, for lamellipodia formation induced by MIM-B.
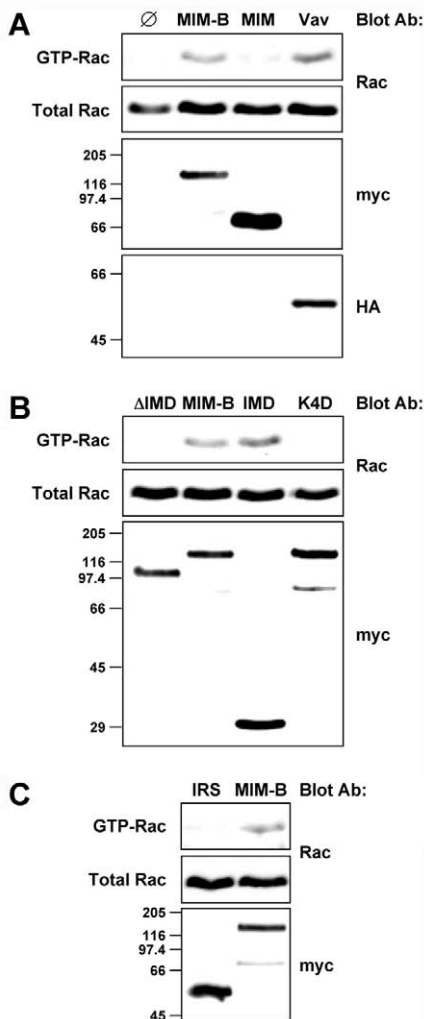
MIM-B binds Rac through its IMD

We demonstrated that the IMD of MIM-B is the minimal sequence required for the activation of Rac. IRSp53 has been previously shown to bind to active Rac through a sequence encompassing the IMD (Miki et al., 2000) and to active Cdc42 through a partial CRIB domain located downstream the IMD (Krugmann et al., 2001). It was speculated that the IMD of

Fig. 5. MIM-B activates Rac through its IMD. (A) MIM-B overexpression activates Rac. Activity of endogenous Rac was determined by pull-down from lysates of COS-7 cells transfected with an empty vector (∅) or constructs encoding myc-MIM-B, myc-MIM or an HA-tagged constitutively active form (DH-PH) of mouse Vav-1 (Vav) using GST-PAK-CRIB. Rac activation was revealed by immunoblotting with anti-Rac antibody. Expression of tagged proteins was subsequently determined by immunoblotting with anti-myc and anti-HA antibodies. (B) The IMD of MIM-B is necessary and sufficient to activate Rac. Rac activity from COS-7 cells overexpressing myc-MIM-B ΔIMD (ΔIMD), myc-MIM-B, myc-IMD or myc-MIM-B K4D (K4D) was determined as described above. (C) IRSp53 does not activate Rac. Rac activity of COS-7 cells expressing myc-IRSp53 (IRS) or myc-MIM-B was determined as above. These results are representative of at least three different experiments.

IRSp53 (and thus probably other IMDs) might bind to Rac via a central patch similar to that on the BAR domain, a closely related structure (Peter et al., 2004). Binding of IMDs to Rac could be a conserved property and might be potentially involved in Rac activation by MIM-B. To investigate MIM-B binding to Rac we performed pull-down experiments using recombinant constitutively active mutant (L61) or dominant-negative mutant (N17) of Rac or Cdc42 fused to GST. Full-length MIM-B interacts with Rac but not Cdc42 mutants (Fig. 6A). This binding is completely prevented by deletion of the IMD, which like the full-length protein, strongly binds only Rac mutants (Fig. 6A). Binding of overexpressed full-length MIM-B to Rac was reduced in normal salt conditions (data not shown) and thus we performed pull downs in low salt conditions (50 mM NaCl). However, we confirmed that endogenous MIM-B protein was specifically retained by recombinant Rac but not Cdc42 mutants in normal salt conditions (Fig. 6B). To determine whether the interaction between the IMD of MIM-B with Rac is direct, we incubated recombinant His-tagged IMD (Fig. 6C, left) with recombinant GST-GTPases. We found that the IMD interacts only with Rac, demonstrating a direct and specific binding between both proteins (Fig. 6C, right). This result demonstrates that MIM-B directly interacts with Rac through its IMD and this binding is correlated with Rac activation.

Fig. 6. MIM-B binds to Rac. (A) MIM-B binds Rac through its IMD. Binding to GTPase mutants was determined by GST pull down. Lysates of COS-7 overexpressing myc-MIM-B, myc-MIM-B ΔIMD, myc-MIM-B K4D, myc-IMD or myc-IMD K4D were incubated with recombinant GST-N17 or -L61-Rac or -Cdc42 in low-salt conditions and binding was determined by immunoblotting with anti-myc antibody. L, lysate. (B) Endogenous MIM-B binds to Rac. Representative pull down experiments performed as described above in normal salt conditions using mouse brain extract as protein source. (C) The MIM-B IMD directly binds to Rac mutants. (Left) Recombinant His-tagged IMDs used for pull-downs with recombinant GTPases were separated on SDS-PAGE and stained with Coomassie Blue. (Right) Recombinant GST-GTPases were incubated with either purified His-IMD wild-type (wt) or K4D and binding was revealed by SDS-PAGE and Coomassie Blue staining.

Characterisation of bundling deficient mutant of MIM-B

We showed that MIM-B activity toward the actin cytoskeleton requires binding to and activation of Rac mediated by its IMD. The IMD being an F-actin bundling domain, we wondered if this activity was required for Rac activation or was participating to a certain extent to the MIM-B effect on actin cytoskeleton. We recently published the crystal structure of the IMD domain of IRSp53 (Millard et al., 2005), a zeppelin shaped dimer, possessing two positively charged regions at both extremities provided by each monomer (Fig. 7A, bold bar). Mutation of lysine residues to glutamic acid within this region completely abrogates F-actin binding and thus bundling (Millard et al., 2005). Sequence alignment of IMDs reveals similar positively charged residues in the IMD of MIM-B. Similarly to IRSp53, we mutated lysine residues (lysines 149, 150, 152 and 153) within this conserved region to aspartic acid (K4D mutations, Fig. 7A) and analysed the consequences on F-actin binding and bundling. His-tagged IMD wt and K4D were purified to homogeneity and F-actin binding was studied by high-speed co-sedimentation assay. A significant amount of wt IMD co-pelleted with the F-actin, demonstrating a direct association between both proteins (Fig. 7B). In contrast, the amount of K4D mutant in the pellet did not increase in the presence of F-actin (Fig. 7B). Thus, K4D mutations impair F-actin binding. To confirm this result, we performed an in vitro actin bundling assay based on a low-speed co-sedimentation
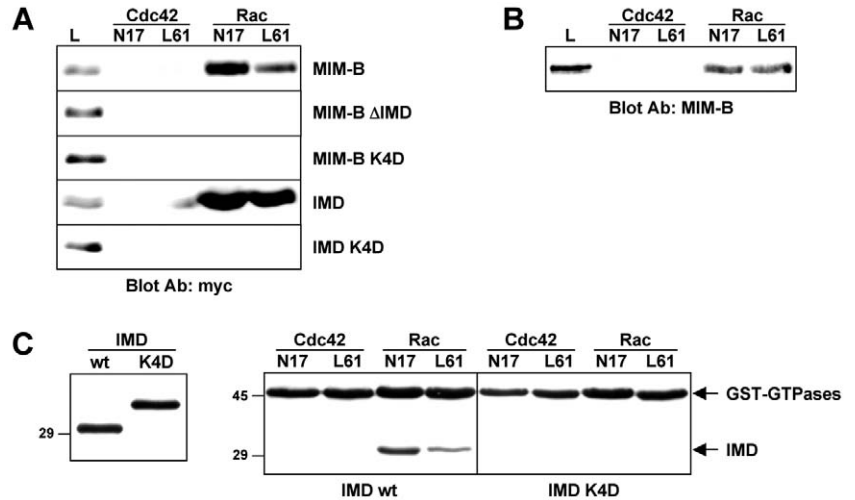
approach (Millard et al., 2005). In the absence of IMD, 25% of F-actin was generally found in the pellet fraction (Fig. 7C). This percentage is greatly enhanced by increasing concentration of wt but not K4D mutant (Fig. 7C). The bundling defect of the K4D mutant was studied in an independent assay in which F-actin coupled to a fluorescent dye (Cy3) (Machesky and Hall, 1997) was incubated with wt or K4D IMD and then visualised by fluorescent light microscopy. The presence of wt IMD resulted in the formation of visible actin bundles whereas nothing was observed with the K4D mutant (Fig. 7D). This result clearly demonstrates the F-actin bundling defect associated with the K4D mutations related to its F-actin binding defect.

In order to confirm that the K4D mutations only affect the F-actin binding and to rule out any effect on IMD structure, we studied the dimerisation status of such a mutant. Indeed, IMD dimerisation is not only required for actin bundling but also allows MIM-B to interact with binding partner such as cortactin (Lin et al., 2005). Myc-tagged IMD wt or K4D were coexpressed with HA-tagged MIM-B, immunoprecipitated and separated onto SDS-PAGE. Immunoblot analysis using an anti-HA antibody reveals an equivalent interaction between MIM-B and either of the IMDs demonstrating that K4D mutations do not affect MIM-B dimerisation.

K4D mutation prevents MIM-B induced cytoskeletal rearrangements, Rac binding and activation

We studied the consequences of K4D mutations on MIM-B activity toward the actin cytoskeleton by expressing a full-

Fig. 7. Characterization of K4D mutant. (A) Alignment of IMD sequences. IMD sequences of IRSp53 (NP_059344), IRTKS (NP_061330), FLJ22582 (NP_079321), MIM-B (AK027015) and ABBA-1 (NP_61239) were aligned using MultAlign (http://prodes.toulouse. inra.fr/multalin/). Symbols above the sequence alignment refer to the secondary structure assignment of IRSp53. Critical basic region of IRSp53 IMD involved in F-actin binding is indicated by a bold bar. Corresponding residues in MIM-B sequence, lysines 149, 150, 152 and 153 mutated to glutamic acids (K4D mutant), are indicated by asterisks. (B) K4D mutations abrogate F-actin binding. Representative high-speed cosedimentation assay of the interaction of 5 μM His-tagged wt or K4D IMD with F-actin (2.5 μM). Results were analysed by SDS-PAGE and Coomassie Blue staining. P, pellet; S, supernatant. (C) K4D mutations prevent F-actin bundling. Various concentrations of His-tagged IMD wt or K4D were incubated with 5 μM F-actin and F-actin bundling was determined by low-speed co-sedimentation assay. F-actin present in the supernatant (S) and pellet (P) fractions was revealed by SDS-PAGE and Coomassie Blue staining. Similar results were independently obtained at least three times. (D) Bundling defect of His-tagged IMD K4D revealed by fluorescence-microscopy-based F-actin-bundling assay. Cy3-labelled F-actin (1 μM) was incubated with 10 μM His-tagged IMD wt or K4D and imaged using a fluorescence microscope. (E) K4D mutations do not affect IMD dimerisation. COS-7 cells were co-transfected with constructs expressing myc-IMD wt or K4D and HA-MIM-B. Myc-tagged proteins were immunoprecipitated with anti-myc antibody and binding to HA-MIM-B was determined by immunoblotting with anti-HA antibody. Expression and immunoprecipitation of myc-tagged protein was subsequently analysed with anti-myc antibody. Bar, 20 μm.

length mutated MIM-B into COS-7 cells. Similarly to Swiss 3T3 cells MIM-B induces actin-rich membrane protrusions at the cell periphery and dense microspike network at cell-cell junctions (Fig. 8A-C, arrowheads). MIM-B also induces the formation of structures resembling apical microvilli in most of the cells (not shown) and reduces stress fibre numbers at high expression level as already observed (Gonzalez-Quevedo et al., 2005; Mattila et al., 2003; Woodings et al., 2003). MIM-B effect toward the actin cytoskeleton with these unpolarised thin lamellipodia is so characteristic that more than 80% of
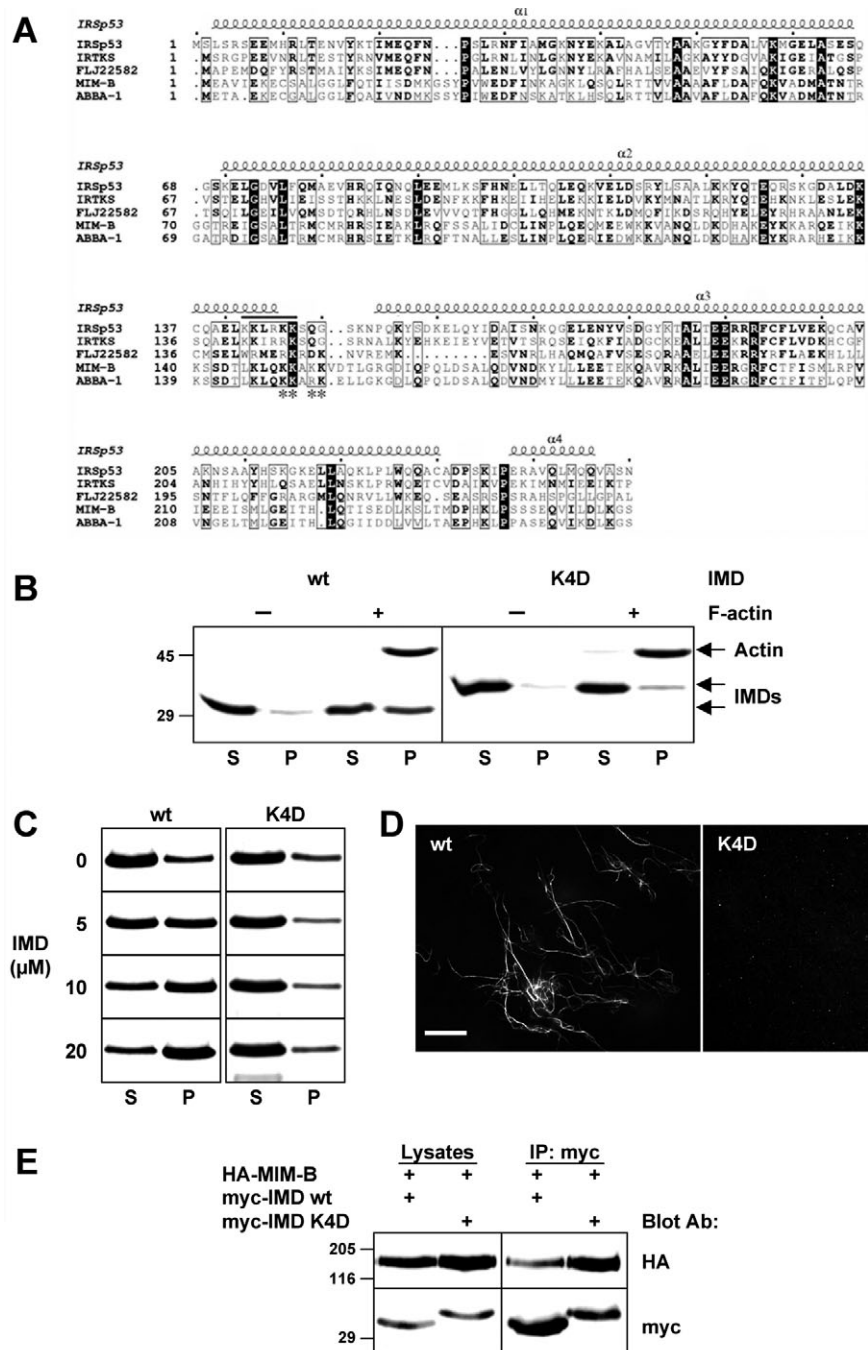
transfected cells can be identified blind, by simply looking at the phalloidin staining. On the contrary, MIM-B K4D has no significant effect on the actin cytoskeleton (Fig. 8D-F) similarly to the deleted IMD mutant (Fig. 8G-I) even if these mutants still localised at the cell periphery and colocalised with certain actin structures (Fig. 8F,I, arrowheads). By blind observation of phalloidin staining, around 10% of MIM-B K4D- or MIM-B ΔIMD-transfected cells have an apparent MIM-B phenotype, which is similar to untransfected cells.

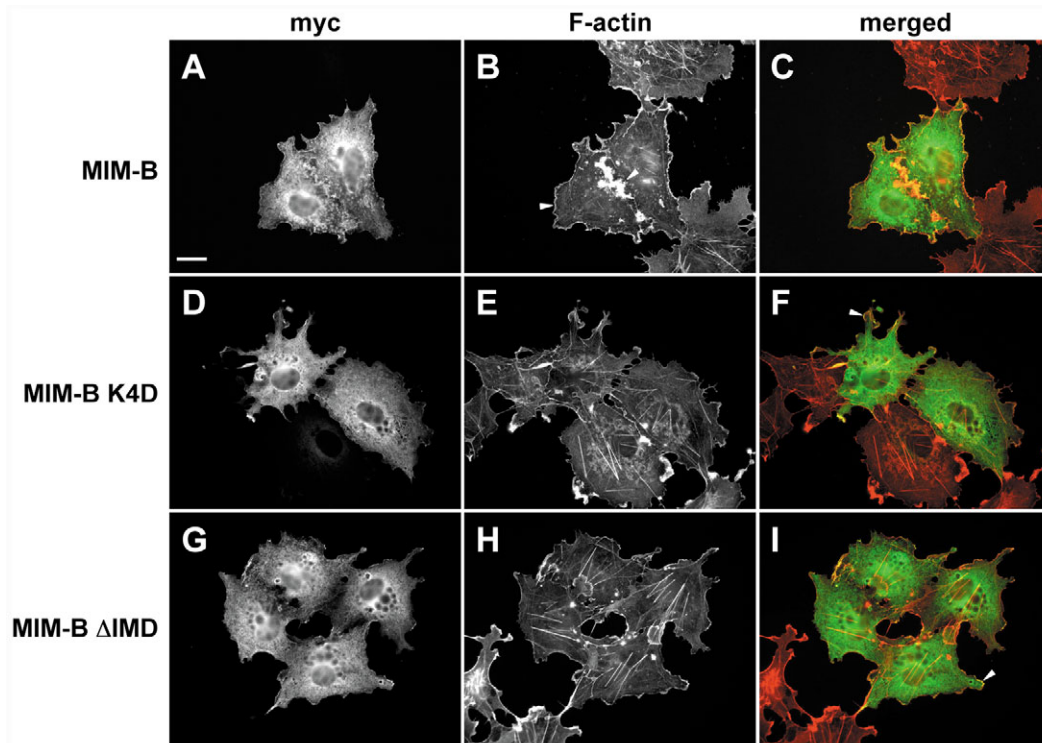This result suggests that the bundling activity of MIM-B is

Fig. 8. K4D mutations inhibits MIM-B activity towards the actin cytoskeleton. COS-7 cells transfected with constructs expressing myc-MIM-B wt (A-C), K4D (D-F) or ΔIMD (G-I) were treated for indirect immunofluorescence as described in Fig. 3. Bar, 10 μm.
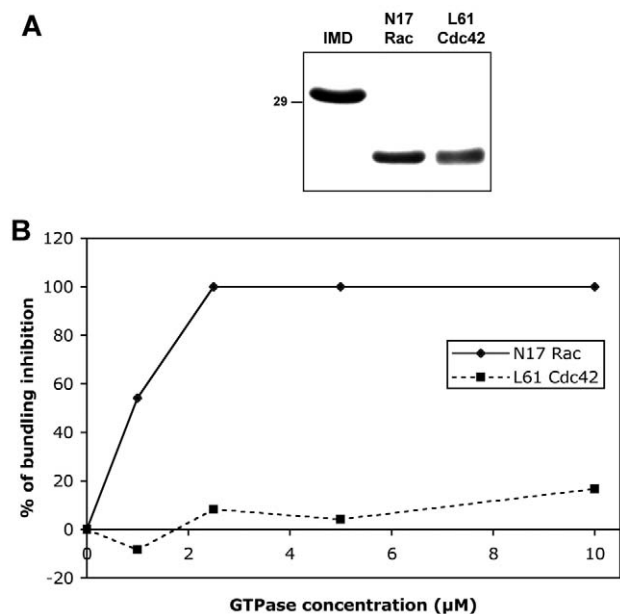
required for its effect on the cytoskeleton or that the K4D mutations affect MIM-B activity towards Rac. In order to investigate this latter possibility we studied the effect of K4D mutations on Rac activation and binding. The mutated form of full-length MIM-B was found to no longer stimulate Rac (Fig. 5B). This defect is correlated by a complete lack of binding of MIM-B K4D or IMD K4D to Rac (Fig. 6A,C) clearly demonstrating that the bundling activity of the IMD is non dissociable from its Rac-stimulating effect.

Rac binding inhibits the F-actin bundling activity of the IMD of MIM-B

As mutations that prevent F-actin bundling of the IMD also affect Rac binding and activation, we wondered whether Rac binding may affect F-actin bundling. Increasing concentrations of purified recombinant GTPases (1-10 μM) were then incubated with 5 μM purified His-tagged IMD before the addition of 5 μM F-actin (Fig. 9A). F-actin bundling was then studied by low-speed co-sedimentation assay. The percentage of F-actin recovered into the pellet was densitometrically

evaluated after separation onto SDS-PAGE. Results were normalised by subtracting the percentage of F-actin associated with pellet in absence of IMD and expressed as a percentage of bundling inhibition. L61-Cdc42 was used as a control as it does not bind to the IMD of MIM-B. In this representative experiment, at a concentration of 2.5 μM N17-Rac completely inhibited the bundling activity of the IMD, while 2.5 μM L61-Cdc42 had no detectable effect (Fig. 9B). This result shows that Rac binding to the IMD inhibits its bundling activity. All together, these data suggest that Rac interaction and actin bundling are functionally connected in MIM-B.

Fig. 9. The F-actin bundling activity of the IMD of MIM-B is inhibited by Rac. (A) Protein used in this assay. Recombinant His-tagged IMD and GTPase mutants were purified to homogeneity and analysed on SDS-PAGE followed by Coomassie Blue staining. Position of molecular size marker in kDa is indicated. (B) In this representative experiment, 5 μM His-tagged IMD (see Fig. 9A) were pre-incubated with various concentrations of recombinant N17-Rac or L61-Cdc42 (see Fig. 9A) before addition of 5 μM F-actin. F-actin bundling was determined as described in Fig. 7. Pellet fractions were analysed by SDS-PAGE and the band intensity of actin was measured densitometrically. Percentage of F-actin bundled was normalised by F-actin bundled in the absence of IMD and expressed as percentage of bundling inhibition.

Discussion

We recently identified MIM-B as a protein potentially involved in the rearrangement of the actin cytoskeleton to establish dynamic actin structures (Woodings et al., 2003). MIM-B is a long isoform of MIM, a potential suppressor of metastasis in bladder cancer (Lee et al., 2002), whose expression has only been studied at the mRNA level (Mattila et al., 2003; Nixdorf et al., 2004). MIM-B has also been implicated in basal cell carcinomas as a sonic hedgehog responsive gene and an enhancer of Gli transcription (Callahan et al., 2004). Through the development of a specific polyclonal anti-MIM-B antibody, we showed that MIM-B protein is widely expressed. Despite the fact that MIM-B mRNA was not detected in two different metastatic cell lines originated from bladder, J82 and TccSup cells, no clear correlation between MIM-B mRNA level and the metastatic status of cells has been clearly demonstrated (Lee et al., 2002; Nixdorf et al., 2004). We did not observe any variation of MIM-B protein expression in multiple bladder cancer cell lines, including J82 and TccSup, but also in prostate and breast cancer cell lines. Our study provides compelling evidence that the expression of MIM-B is not dependent on the metastatic status of cells and MIM-B is therefore unlikely to be a suppressor of metastasis, whereas the question remains open for MIM.

As MIM-B binds monomeric and filamentous actin, we sought to evaluate the contribution of each interaction to MIM-B activity in cells. We demonstrated that the IMD, but not the WH2 motif, is required for actin-rich membrane protrusions induced by MIM-B suggesting an important role of binding and bundling of filamentous actin. Although the IMD of MIM-B was sufficient to elicit cell morphological changes similar to other IMDs (Yamagishi et al., 2004) it was not sufficient to induce lamellipodia in serum-starved cells; C-terminal sequences were also required (see below). Our results also demonstrate that MIM-B activates Rac through its IMD, and that Rac activation is necessary for the lamellipodial protrusions of cells expressing full-length MIM-B but not the spiky appearance of cells transfected with the IMD alone. The mechanisms of Rac activation by the IMD are unknown, and this activity does not seem to be conserved in IRSp53, confirming previous observations (Funato et al., 2004). We wondered whether the IMD was a GTP exchange factor (GEF), despite the lack of domain conservation between the IMD and GEFs, as Rac interacts directly with the IMD of MIM-B. Through an in vitro exchange assay we were however unable to detect any GDP to GTP exchange on Rac induced by the IMD (G.B. and A. Schimdt, unpublished), suggesting that the IMD is not a GEF. This idea is reinforced by the fact that the IMD binds Rac in an apparent GTP-independent manner, where GEF preferentially interact with GDP-loaded GTPases (Schmidt and Hall, 2002). It is therefore possible that the IMD acts as a scaffold protein that binds Rac and a GEF, facilitating Rac activation. We thus examined the binding of MIM-B to various Rac-GEFs (Trio, Tiam1, SOS-1 and Vav1) by co-immunoprecipitation but could not identify any interaction (G.B. and L.M.M., unpublished). Thus, there may still be a GEF that we haven't yet tested or the IMD may function by altering other interactions of Rac to promote activation.

Overexpression of the IMD of MIM-B has been shown to induce long actin-rich processes that look like filopodia (Yamagishi et al., 2004). Although the IMD is necessary and sufficient to activate Rac, it does not induce lamellipodia formation. Mislocalisation of activated Rac or mislocalised activation of Rac could prevent or inhibit some Rac activities toward the actin cytoskeleton. For example, it has recently been shown that disruption of dynamin activity prevents lamellipodia formation induced during spreading or by growth factors despite Rac activation (Schlunck et al., 2004). Mislocalisation of Rac by dynamin inhibition is responsible of such a phenotype (Schlunck et al., 2004). It is therefore possible that the IMD alone can activate Rac but in a lamellipodia-unproductive localisation preventing interaction with critical Rac effectors. Actin rearrangements induced by the IMD could thus result from mislocalisation of Rac activity and/or from the bundling activity of this domain.

Our data suggest that a region between the IMD and the WH2 motif is required for MIM-B to induce lamellipodia-like structures. Our preliminary data show that residues 261 to 403 are dispensable, but residues 599 to 727 are required, for MIM-B induced actin-rich membrane protrusions in agreement with previous observations (Woodings et al., 2003). MIM-B could thus act as a scaffold protein, which organises spatiotemporally a group of proteins with related functions within the confines of a cell. A growing body of evidence suggests that certain GEFs contribute to the selection of a subset of GTPase effectors through binding to such scaffold proteins which complex with components of specific GTPase effector pathways (Buchsbaum et al., 2002; Buchsbaum et al., 2003; Connolly et al., 2005; Jaffe et al., 2005). In addition to participating to Rac activation, MIM-B could thus link activated Rac to certain targets involved in lamellipodia formation, such as WAVE/SCAR proteins, which activate the Arp2/3 complex (Bompard and Caron, 2004; Millard et al., 2004).

Cortactin is another nucleation promoting factor whose activity toward the Arp2/3 complex is greatly enhanced after MIM-B binding (Lin et al., 2005). Cortactin plays an important role in lamellipodia/ruffle structures presumably by enhancing the formation of a branched actin network and/or stabilising networks induced by WAVE/SCAR proteins (Daly, 2004). A MIM-B mutant lacking the proline-rich region inhibits MIM-B enhanced cell migration presumably by preventing cortactin binding (Lin et al., 2005) and we found that a similar mutant is deficient in lamellipodia formation (G.B. and L.M.M., unpublished). A role of cortactin in actin-rich membrane protrusions induced by MIM-B is suggested by the colocalisation of endogenous cortactin with MIM-B within such structures (G.B. and L.M.M., unpublished).

Our results demonstrate that the IMD of MIM-B plays an important role in MIM-B activity toward the actin cytoskeleton. As discussed before, the IMD induces Rac activation and actin bundling. In an attempt to define if the bundling activity of the IMD was required for Rac activation or was participating to cytoskeletal rearrangements induced by MIM-B, we mutated conserved residues involved in F-actin binding on the basis of the crystal structure of the IMD of IRSp53 (Millard et al., 2005). As expected, these mutations (K4D) prevent actin binding and bundling by the IMD, but surprisingly also inhibit Rac binding and activation rendering the separation of both activities impossible. This could be interpreted in at least two different ways. First of all, the F-actin and Rac binding sites on the IMD are similar or

overlapping. Alternatively, the Rac binding site on the IMD is unique but rendered inaccessible by the negative charge introduced in the K4D mutant. Our results cannot distinguish between these hypotheses at this point. Finally, we found that the bundling activity of the IMD is inhibited by Rac binding, suggesting that both activities are exclusive. The inhibition of the bundling activity of the IMD by Rac binding could play an important role in the establishment of lamellipodia formation by MIM-B (Millard et al., 2004; Pollard and Borisy, 2003). Our results may also have strong implications for the interpretation of our previous observations concerning the IMD domain of IRSp53 (Millard et al., 2005), as we found that its bundling activity is also inhibited by Rac under our new conditions and that the mutant deficient for F-actin binding (K142,143,146,147E) does not interact with Rac (G.B., T. H. Millard and L.M.M., unpublished). Thus, we believe that the Rac binding and actin binding are intimately connected in IMD proteins and may have close proximity binding sites.

In conclusion, we show that MIM-B expression in cells induces Rac activation and lamellipodia formation. Although the IMD of MIM-B is sufficient to interact with Rac, and to promote Rac activation in cells, it does not provoke lamellipodia assembly. Other regions of MIM-B and other protein interactions are probably required: MIM-B thus acting as scaffold protein. Furthermore, we established that the actin-bundling and Rac-binding properties of MIM-B are not separable, calling into question current proposals for how IMD proteins bundle actin filaments and the importance of bundling for filopodia assembly.

References

Bompard, G. and Caron, E. (2004). Regulation of WASP/WAVE proteins: making a long story short. *J. Cell Biol.* **166**, 957-962.

Buchsbaum, R. J., Connolly, B. A. and Feig, L. A. (2002). Interaction of Rac exchange factors Tiam1 and Ras-GRF1 with a scaffold for the p38 mitogen-activated protein kinase cascade. *Mol. Cell. Biol.* **22**, 4073-4085.

Buchsbaum, R. J., Connolly, B. A. and Feig, L. A. (2003). Regulation of p70 S6 kinase by complex formation between the Rac guanine nucleotide exchange factor (Rac-GEF) Tiam1 and the scaffold spinophilin. *J. Biol. Chem.* **278**, 18833-18841.

Callahan, C. A., Ofstad, T., Horng, L., Wang, J. K., Zhen, H. H., Coulombe, P. A. and Oro, A. E. (2004). MIM/BEG4, a Sonic hedgehog-responsive gene that potentiates Gli-dependent transcription. *Genes Dev.* **18**, 2724-2729.

Connolly, B. A., Rice, J., Feig, L. A. and Buchsbaum, R. J. (2005). Tiam1-IRSp53 complex formation directs specificity of Rac-mediated actin cytoskeleton regulation. *Mol. Cell. Biol.* **25**, 4602-4614.

Daly, R. J. (2004). Cortactin signalling and dynamic actin networks. *Biochem. J.* **382**, 13-25.

Etienne-Manneville, S. and Hall, A. (2002). Rho GTPases in cell biology. *Nature* **420**, 629-635.

Funato, Y., Terabayashi, T., Suenaga, N., Seiki, M., Takenawa, T. and Miki, H. (2004). IRSp53/Eps8 complex is important for positive regulation of Rac and cancer cell motility/invasiveness. *Cancer Res.* **64**, 5237-5244.

Gonzalez-Quevedo, R., Shoffer, M., Horng, L. and Oro, A. E. (2005). Receptor tyrosine phosphatase-dependent cytoskeletal remodeling by the hedgehog-responsive gene MIM/BEG4. *J. Cell Biol.* **168**, 453-463.

Hall, A. (1994). Small GTP-binding proteins and the regulation of the actin cytoskeleton. *Annu. Rev. Cell Biol.* **10**, 31-54.

Hall, A. (1998). Rho GTPases and the actin cytoskeleton. *Science* **279**, 509-514.

Jaffe, A. B., Hall, A. and Schmidt, A. (2005). Association of CNK1 with Rho guanine nucleotide exchange factors controls signaling specificity downstream of Rho. *Curr. Biol.* **15**, 405-412.

Krugmann, S., Jordens, I., Gevaert, K., Driessens, M., Vandekerckhove, J. and Hall, A. (2001). Cdc42 induces filopodia by promoting the formation of an IRSp53:Mena complex. *Curr. Biol.* **11**, 1645-1655.

Lee, Y. G., Macoska, J. A., Korenchuk, S. and Pienta, K. J. (2002). MIM, a potential metastasis suppressor gene in bladder cancer. *Neoplasia* **4**, 291-294.

Lin, J., Liu, J., Wang, Y., Zhu, J., Zhou, K., Smith, N. and Zhan, X. (2005). Differential regulation of cortactin and N-WASP-mediated actin polymerization by missing in metastasis (MIM) protein. *Oncogene* **24**, 2059-2066.

Loberg, R. D., Neeley, C. K., Adam-Day, L. L., Fridman, Y., St John, L. N., Nixdorf, S., Jackson, P., Kalikin, L. M. and Pienta, K. J. (2005). Differential expression analysis of MIM (MTSS1) splice variants and a functional role of MIM in prostate cancer cell biology. *Int. J. Oncol.* **26**, 1699-1705.

Machesky, L. M. and Hall, A. (1997). Role of actin polymerization and adhesion to extracellular matrix in Rac- and Rho-induced cytoskeletal reorganization. *J. Cell Biol.* **138**, 913-926.

Mattila, P. K., Salminen, M., Yamashiro, T. and Lappalainen, P. (2003). Mouse MIM, a tissue-specific regulator of cytoskeletal dynamics, interacts with ATP-actin monomers through its C-terminal WH2 domain. *J. Biol. Chem.* **278**, 8452-8459.

Miki, H., Yamaguchi, H., Suetsugu, S. and Takenawa, T. (2000). IRSp53 is an essential intermediate between Rac and WAVE in the regulation of membrane ruffling. *Nature* **408**, 732-735.

Millard, T. H., Sharp, S. J. and Machesky, L. M. (2004). Signalling to actin assembly via the WASP-family proteins and the Arp2/3 complex. *Biochem. J.* **380**, 1-17.

Millard, T. H., Bompard, G., Heung, M. Y., Dafforn, T. R., Scott, D. J., Machesky, L. M. and Futterer, K. (2005). Structural basis of filopodia formation induced by the IRSp53/MIM homology domain of human IRSp53. *EMBO J.* **24**, 240-250.

Nixdorf, S., Grimm, M. O., Loberg, R., Marreiros, A., Russell, P. J., Pienta, K. J. and Jackson, P. (2004). Expression and regulation of MIM (Missing In Metastasis), a novel putative metastasis suppressor gene, and MIM-B, in bladder cancer cell lines. *Cancer Lett.* **215**, 209-220.

Paavilainen, V. O., Bertling, E., Falck, S. and Lappalainen, P. (2004). Regulation of cytoskeletal dynamics by actin-monomer-binding proteins. *Trends Cell. Biol.* **14**, 386-394.

Peter, B. J., Kent, H. M., Mills, I. G., Vallis, Y., Butler, P. J., Evans, P. R. and McMahon, H. T. (2004). BAR domains as sensors of membrane curvature: the amphiphysin BAR structure. *Science* **303**, 495-499.

Pollard, T. D. (1984). Purification of a high molecular weight actin filament gelation protein from Acanthamoeba that shares antigenic determinants with vertebrate spectrins. *J. Cell Biol.* **99**, 1970-1980.

Pollard, T. D. and Borisy, G. G. (2003). Cellular motility driven by assembly and disassembly of actin filaments. *Cell* **112**, 453-465.

Revenu, C., Athman, R., Robine, S. and Louvard, D. (2004). The co-workers of actin filaments: from cell structures to signals. *Nat. Rev. Mol. Cell. Biol.* **5**, 635-646.

Schlunck, G., Damke, H., Kiosses, W. B., Rusk, N., Symons, M. H., Waterman-Storer, C. M., Schmid, S. L. and Schwartz, M. A. (2004). Modulation of Rac localization and function by dynamin. *Mol. Biol. Cell* **15**, 256-267.

Schmidt, A. and Hall, A. (2002). Guanine nucleotide exchange factors for Rho GTPases: turning on the switch. *Genes Dev.* **16**, 1587-1609.

Woodings, J. A., Sharp, S. J. and Machesky, L. M. (2003). MIM-B, a putative metastasis suppressor protein, binds to actin and to protein tyrosine phosphatase delta. *Biochem. J.* **371**, 463-471.

Yamagishi, A., Masuda, M., Ohki, T., Onishi, H. and Mochizuki, N. (2004). A novel actin bundling/filopodium-forming domain conserved in insulin receptor tyrosine kinase substrate p53 and missing in metastasis protein. *J. Biol. Chem.* **279**, 14929-14936.